

# TECHNICAL REPORT

**Methods of measurement of the magnetic properties of permanent magnet (magnetically hard) materials in an open magnetic circuit using a superconducting magnet**

IECNORM.COM : Click to view the full PDF of IEC TR 63304:2021



**THIS PUBLICATION IS COPYRIGHT PROTECTED**  
**Copyright © 2021 IEC, Geneva, Switzerland**

All rights reserved. Unless otherwise specified, no part of this publication may be reproduced or utilized in any form or by any means, electronic or mechanical, including photocopying and microfilm, without permission in writing from either IEC or IEC's member National Committee in the country of the requester. If you have any questions about IEC copyright or have an enquiry about obtaining additional rights to this publication, please contact the address below or your local IEC member National Committee for further information.

IEC Central Office  
3, rue de Varembe  
CH-1211 Geneva 20  
Switzerland

Tel.: +41 22 919 02 11  
[info@iec.ch](mailto:info@iec.ch)  
[www.iec.ch](http://www.iec.ch)

**About the IEC**

The International Electrotechnical Commission (IEC) is the leading global organization that prepares and publishes International Standards for all electrical, electronic and related technologies.

**About IEC publications**

The technical content of IEC publications is kept under constant review by the IEC. Please make sure that you have the latest edition, a corrigendum or an amendment might have been published.

**IEC publications search - [webstore.iec.ch/advsearchform](http://webstore.iec.ch/advsearchform)**

The advanced search enables to find IEC publications by a variety of criteria (reference number, text, technical committee, ...). It also gives information on projects, replaced and withdrawn publications.

**IEC Just Published - [webstore.iec.ch/justpublished](http://webstore.iec.ch/justpublished)**

Stay up to date on all new IEC publications. Just Published details all new publications released. Available online and once a month by email.

**IEC Customer Service Centre - [webstore.iec.ch/csc](http://webstore.iec.ch/csc)**

If you wish to give us your feedback on this publication or need further assistance, please contact the Customer Service Centre: [sales@iec.ch](mailto:sales@iec.ch).

**IEC online collection - [oc.iec.ch](http://oc.iec.ch)**

Discover our powerful search engine and read freely all the publications previews. With a subscription you will always have access to up to date content tailored to your needs.

**Electropedia - [www.electropedia.org](http://www.electropedia.org)**

The world's leading online dictionary on electrotechnology, containing more than 22 000 terminological entries in English and French, with equivalent terms in 18 additional languages. Also known as the International Electrotechnical Vocabulary (IEV) online.

IECNORM.COM : Click to view the full PDF IEC 603304:2021

# TECHNICAL REPORT

---

**Methods of measurement of the magnetic properties of permanent magnet (magnetically hard) materials in an open magnetic circuit using a superconducting magnet**

INTERNATIONAL  
ELECTROTECHNICAL  
COMMISSION

---

ICS 17.220.20; 29.030

ISBN 978-2-8322-9714-8

**Warning! Make sure that you obtained this publication from an authorized distributor.**

## CONTENTS

FOREWORD.....	5
INTRODUCTION.....	7
1 Scope.....	9
2 Normative references .....	9
3 Terms and definitions .....	9
4 General principle .....	11
4.1 Principle of the method .....	11
4.2 Superconducting magnet (SCM).....	12
4.3 Magnetic field strength sensor ( <i>H</i> sensor).....	13
4.4 Magnetic dipole moment detection coil ( <i>M</i> coil).....	13
4.5 Specimen rod and moving device.....	14
4.6 Measuring devices and the data processing device.....	14
5 Test specimen .....	14
6 Preparation of measurement.....	15
6.1 Measurement of volume of the test specimen.....	15
6.2 Initial magnetization of the test specimen to saturation .....	15
7 Determination of magnetic polarization .....	15
7.1 Measurement of the magnetic dipole moment.....	15
7.2 Determination of magnetic polarization .....	16
8 Measurement of magnetic field .....	17
9 Calibration of the magnetic dipole moment detection coil ( <i>M</i> coil).....	17
10 Determination of demagnetization curve.....	17
11 Demagnetizing field correction.....	18
11.1 General.....	18
11.2 Method A: Method using a demagnetizing factor determined by the shape of the test specimen only .....	20
11.3 Method B: Method using a demagnetizing factor determined by the shape and the magnetic susceptibility of the test specimen .....	20
11.4 Method C: Method using an inverse analysis considering the spatial distribution of the self-demagnetizing field strength in the test specimen.....	21
12 Determination of principal magnetic properties .....	21
12.1 Remanent magnetic polarization $J_r$ .....	21
12.2 Maximum energy product $(BH)_{max}$ .....	22
12.3 Coercivity ( $H_{cJ}$ and $H_{cB}$ ).....	22
13 Reproducibility.....	22
14 Test report.....	22
Annex A (informative) SCM-Magnetometer method .....	24
Annex B (informative) Effects of the test specimen dimensions .....	26
Annex C (informative) Superconducting magnets (SCMs) .....	27
Annex D (informative) Magnetic dipole moment detection coils ( <i>M</i> coils).....	29
Annex E (informative/normative) Details of the demagnetizing field correction .....	31
E.1 General.....	31
E.2 Symbols.....	31

E.3	Method using a demagnetizing factor determined by the shape and magnetic susceptibility of the test specimen (Method B).....	32
E.4	Method using an inverse analysis considering the spatial distribution of the self-demagnetizing field strength in the test specimen (Method C) .....	34
Annex F (informative) Result of the international round robin test of magnetic properties of permanent magnets using the SCM-VSM and SCM-Extraction methods .....		39
F.1	General.....	39
F.2	Protocol of the RRT .....	39
F.3	Result of the RRT .....	40
F.4	Reproducibility of the measurements .....	43
Bibliography.....		45
Figure 1	– Demagnetization curve $J(H)$ .....	10
Figure 2	– Schematic diagrams of the test apparatus.....	11
Figure 3	– Schematic diagrams of the first order gradiometer coil .....	13
Figure 4	– Relationship between magnetic polarization and self-demagnetizing field .....	18
Figure 5	– Schematic diagram of the demagnetizing field correction.....	19
Figure 6	– Conceptual diagram of the procedure of Method C.....	21
Figure A.1	– Schematic diagram of the test apparatus for the SCM-Magnetometer method .....	24
Figure A.2	– Schematic diagrams of the test apparatus for the method in a closed magnetic circuit in accordance with IEC 60404-5 .....	25
Figure B.1	– Effects of test specimen dimensions on magnetic properties [ $B_r$ , $H_{cJ}$ , $H_{cB}$ and $(BH)_{max}$ ] for Nd-Fe-B sintered magnets with different coercivities .....	26
Figure C.1	– Typical cross-sectional structure of the ceramic SCM .....	28
Figure D.1	– Schematic diagram of the second order gradiometer coil for the SCM-VSM method .....	29
Figure D.2	– Schematic diagram of the dependence of induced voltage on the position of the test specimen in the SCM-Extraction method .....	30
Figure E.1	– Axes of a cuboid magnet.....	32
Figure E.2	– Conceptual diagram of the procedure of Method C.....	35
Figure E.3	– Flowchart of the procedure of Method C .....	36
Figure E.4	– Comparison of the demagnetization curves corrected using demagnetizing field correction Methods A, B and C .....	38
Figure F.1	– Comparison of $J_r$ measured by the laboratories.....	40
Figure F.2	– Comparison of $H_{cJ}$ measured by the laboratories .....	41
Figure F.3	– Comparison of $(BH)_{max}$ measured by the laboratories .....	41
Figure F.4	– Comparison of hysteresis loops measured by the laboratories .....	43
Figure F.5	– Relative standard deviation of $J_r$ , $H_{cJ}$ and $(BH)_{max}$ .....	44
Table 1	– Features of the demagnetizing field correction methods in comparison with Method B .....	20
Table 2	– Reproducibility of the magnetic properties .....	22

Table C.1 – Performance of SCMs .....	27
Table F.1 – Nominal values of coercivity .....	39
Table F.2 – Participating laboratories and their employed measuring methods.....	40
Table F.3 – Comparison of magnetic properties measured by the laboratories .....	42
Table F.4 – Comparison of the reproducibility .....	44

IECNORM.COM : Click to view the full PDF of IEC TR 63304:2021

## INTERNATIONAL ELECTROTECHNICAL COMMISSION

## METHODS OF MEASUREMENT OF THE MAGNETIC PROPERTIES OF PERMANENT MAGNET (MAGNETICALLY HARD) MATERIALS IN AN OPEN MAGNETIC CIRCUIT USING A SUPERCONDUCTING MAGNET

### FOREWORD

- 1) The International Electrotechnical Commission (IEC) is a worldwide organization for standardization comprising all national electrotechnical committees (IEC National Committees). The object of IEC is to promote international co-operation on all questions concerning standardization in the electrical and electronic fields. To this end and in addition to other activities, IEC publishes International Standards, Technical Specifications, Technical Reports, Publicly Available Specifications (PAS) and Guides (hereafter referred to as "IEC Publication(s)"). Their preparation is entrusted to technical committees; any IEC National Committee interested in the subject dealt with may participate in this preparatory work. International, governmental and non-governmental organizations liaising with the IEC also participate in this preparation. IEC collaborates closely with the International Organization for Standardization (ISO) in accordance with conditions determined by agreement between the two organizations.
- 2) The formal decisions or agreements of IEC on technical matters express, as nearly as possible, an international consensus of opinion on the relevant subjects since each technical committee has representation from all interested IEC National Committees.
- 3) IEC Publications have the form of recommendations for international use and are accepted by IEC National Committees in that sense. While all reasonable efforts are made to ensure that the technical content of IEC Publications is accurate, IEC cannot be held responsible for the way in which they are used or for any misinterpretation by any end user.
- 4) In order to promote international uniformity, IEC National Committees undertake to apply IEC Publications transparently to the maximum extent possible in their national and regional publications. Any divergence between any IEC Publication and the corresponding national or regional publication shall be clearly indicated in the latter.
- 5) IEC itself does not provide any attestation of conformity. Independent certification bodies provide conformity assessment services and, in some areas, access to IEC marks of conformity. IEC is not responsible for any services carried out by independent certification bodies.
- 6) All users should ensure that they have the latest edition of this publication.
- 7) No liability shall attach to IEC or its directors, employees, servants or agents including individual experts and members of its technical committees and IEC National Committees for any personal injury, property damage or other damage of any nature whatsoever, whether direct or indirect, or for costs (including legal fees) and expenses arising out of the publication, use of, or reliance upon, this IEC Publication or any other IEC Publications.
- 8) Attention is drawn to the Normative references cited in this publication. Use of the referenced publications is indispensable for the correct application of this publication.
- 9) Attention is drawn to the possibility that some of the elements of this IEC Publication may be the subject of patent rights. IEC shall not be held responsible for identifying any or all such patent rights.

IEC TR 63304 has been prepared by IEC technical committee 68: Magnetic alloys and steels. It is a Technical Report.

The text of this Technical Report is based on the following documents:

DTR	Report on voting
68/675/DTR	68/680/RVDTR

Full information on the voting for its approval can be found in the report on voting indicated in the above table.

The language used for the development of this Technical Report is English.

This document was drafted in accordance with ISO/IEC Directives, Part 2, and developed in accordance with ISO/IEC Directives, Part 1 and ISO/IEC Directives, IEC Supplement, available at [www.iec.ch/members\\_experts/refdocs](http://www.iec.ch/members_experts/refdocs). The main document types developed by IEC are described in greater detail at [www.iec.ch/standardsdev/publications](http://www.iec.ch/standardsdev/publications).

The committee has decided that the contents of this document will remain unchanged until the stability date indicated on the IEC website under [webstore.iec.ch](http://webstore.iec.ch) in the data related to the specific document. At this date, the document will be

- reconfirmed,
- withdrawn,
- replaced by a revised edition, or
- amended.

IECNORM.COM : Click to view the full PDF of IEC TR 63304:2021

## INTRODUCTION

Permanent magnet materials with high coercivity e.g. Nd-Fe-B magnets, have been used in industry and its usage increases rapidly to meet demands to improve energy saving and to increase efficiency of electromagnetic applications, e.g. traction motors for Electric Vehicle (EV) and Hybrid Electric Vehicle (HEV).

However, there is no standard method which can determine all the magnetic properties of the permanent magnet materials with coercivity  $H_{cJ}$  higher than 2 MA/m. The method specified in IEC 60404-5, which is a method of measurement in a closed magnetic circuit, can lead to significant measurement errors for measurement of  $H_{cJ} \geq 1,6$  MA/m due to magnetic saturation in parts of the pole faces of the yoke (see IEC 60404-5).

In order to solve the problem, several methods of measurement in an open magnetic circuit using a superconducting magnet (SCM) without a yoke have been developed. The methods using a SCM have been considered to be candidates for solution to accurate measurement of high performance permanent magnets.

The method using a conventional SCM made of metallic superconducting coil has not been used widely for industrial applications due to costs for using expensive liquid helium, limited speed of variation of magnetic field strength, and the difficulty to deal with test specimens of industrial size.

However, nowadays these problems have been solved thanks to the development of a ceramic SCM made of ceramic high temperature superconducting coil. This method has enabled the higher speed of variation of magnetic field strength without using precious resource of liquid helium (see Annex C). Furthermore, test apparatus using the ceramic SCM which can treat test specimens of industrial size have been commercialized globally for industrial use.

However, results of measurement in an open magnetic circuit are different from those of measurement in accordance with IEC 60404-5, particularly in terms of the squareness of demagnetization curves. This is caused by the influence of the self-demagnetizing field in the test specimen, which is opposed to magnetization. This is particular to the measurement in an open magnetic circuit. Therefore, a correction of the influence of self-demagnetizing field (demagnetizing field correction) on the demagnetization curve measured in an open magnetic circuit is indispensable.

This document describes three methods of measurement in an open magnetic circuit using a superconducting magnet (SCM), as follows:

- a) SCM-Vibrating Sample Magnetometer (VSM) method;
- b) SCM-Extraction method;
- c) SCM-Magnetometer method.

In these methods, a test specimen is placed in a detection coil placed in a uniform magnetic field generated by a SCM. For methods a) and b), the magnetic dipole moment of the test specimen is detected by voltage induced in the detection coil due to a vibration and an extraction of the test specimen, respectively. For the method c), a variation of magnetic polarization of a stationary test specimen is detected by voltage induced in the detection coil due to a variation of the magnetic field strength applied to the test specimen.

The reproducibility of measurements of the methods a) and b) has been confirmed by an international round robin test (RRT) that was comparable with that of IEC 60404-5 (see Annex F). However, the reproducibility of the method c) has not been confirmed by a RRT yet. Therefore, the method c) is described separately in Annex A.

There is another method of the measurement in an open magnetic circuit, i.e. the pulsed field magnetometer (PFM), which is described in IEC TR 62331 [1]<sup>1</sup>. The PFM is different from the methods described in this document. The PFM measures a steep AC magnetic response of a test specimen in a pulsed current magnetic field. Consequently, additional correction is indispensable due to the influence of eddy currents in the test specimen and the magnetic viscosity of the magnetic materials.

A demagnetization curve should be measured by decreasing the magnetic field strength with a sufficiently slow speed during the reversal of the polarization to avoid significant magnetic viscosity and eddy current effects in accordance with IEC 60404-5. In the case of adopting a conventional metallic SCM made of metallic superconducting coil, the speed of variation of the magnetic field is too slow so that it takes an hour to obtain a demagnetization curve because of a limit of variation rate of the magnetic field to maintain the coil in a superconducting state. The problem has been solved by adopting a newly developed ceramic SCM made of ceramic high temperature superconducting coil so that a demagnetization curve can be measured within several minutes (see Annex C).

A new method of the demagnetizing field correction has been developed (see Annex E). It is a finite element method (FEM) considering the spatial distribution of self-demagnetizing field strength in the test specimen. The squareness of the corrected demagnetization curve is comparable with that measured in accordance with IEC 60404-5.

---

<sup>1</sup> Numbers in square brackets refer to the Bibliography.

# METHODS OF MEASUREMENT OF THE MAGNETIC PROPERTIES OF PERMANENT MAGNET (MAGNETICALLY HARD) MATERIALS IN AN OPEN MAGNETIC CIRCUIT USING A SUPERCONDUCTING MAGNET

## 1 Scope

This Technical Report describes the general principle and technical details of the methods of measurement of the DC magnetic properties of permanent magnet materials in an open magnetic circuit using a superconducting magnet (SCM).

This method is applicable to permanent magnet materials, such as those specified in IEC 60404-8-1, the properties of which are presumed homogeneous throughout their volume.

There are two methods:

- the SCM-Vibrating Sample Magnetometer (VSM) method;
- the SCM-Extraction method.

This document also describes methods to correct the influence of the self-demagnetizing field in the test specimen on the demagnetization curve measured in an open magnetic circuit. The magnetic properties are determined from the corrected demagnetization curve.

NOTE These SCM-methods can determine the magnetic properties of permanent magnet materials with coercivity higher than 2 MA/m. The methods of measurement in a closed magnetic circuit specified in IEC 60404-5 can lead to significant measurement error due to saturation effects in the pole pieces of yoke for the magnetic materials with coercivity higher than 1,6 MA/m (see IEC 60404-5).

## 2 Normative references

The following documents are referred to in the text in such a way that some or all of their content constitutes requirements of this document. For dated references, only the edition cited applies. For undated references, the latest edition of the referenced document (including any amendments) applies.

IEC 60404-5, *Magnetic materials – Part 5: Permanent magnet (magnetically hard) materials – Methods of measurement of magnetic properties*

IEC 60404-8-1, *Magnetic materials – Part 8-1: Specifications for individual materials – Magnetically hard materials*

IEC 60050-121, *International Electrotechnical Vocabulary – Part 121: Electromagnetism*

IEC 60050-151, *International Electrotechnical Vocabulary – Part 151: Electrical and magnetic devices*

IEC 60050-221, *International Electrotechnical Vocabulary – Chapter 221: Magnetic materials and components*

## 3 Terms and definitions

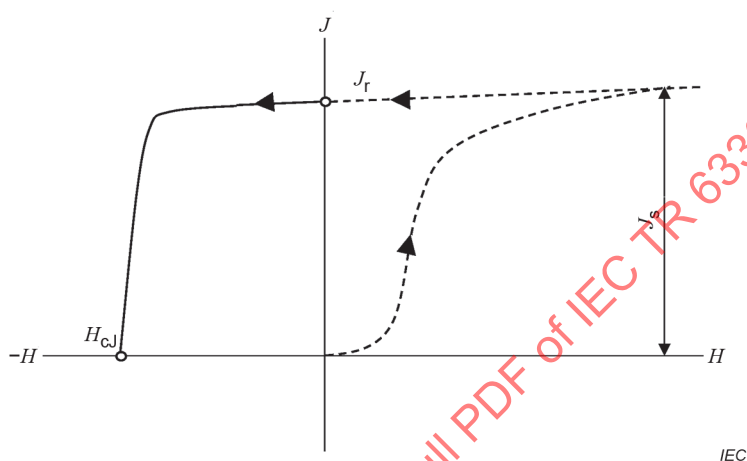
For the purposes of this document, the terms and definitions given in IEC 60050-121, IEC 60050-151, IEC 60050-221 and the following apply.

ISO and IEC maintain terminological databases for use in standardization at the following addresses:

- IEC Electropedia: available at <http://www.electropedia.org/>
- ISO Online browsing platform: available at <http://www.iso.org/obp>

**3.1 demagnetization curve**

part of a hysteresis loop in which the magnetic polarization goes from the remanent magnetic polarization to zero when the applied magnetic field strength varies monotonically, as illustrated in Figure 1



**Key**

- $J_s$  saturation magnetic polarization, in T
- $J_r$  remanent magnetic polarization, in T
- $H_{cJ}$  coercivity relating to the magnetic polarization, in A/m

**Figure 1 – Demagnetization curve  $J(H)$**

Note 1 to entry: A demagnetization curve can be measured from near magnetic saturation.

[SOURCE: IEC 60050-121:1998, 121-12-72, modified – magnetic flux density is replaced by magnetic polarization and Note 1 to entry and Figure 1 have been added]

**3.2 magnetic dipole moment**

$m$

vector quantity given by the volume integral of the magnetic polarization

[SOURCE: IEC 60050-221:1990, 221-01-07, modified – the symbol  $j$  is changed to  $m$  which is used industrially and the note has been removed]

**3.3 M coil**

detection coil for magnetic dipole moment

**3.4 J coil**

detection coil for magnetic polarization

## 4 General principle

### 4.1 Principle of the method

Figure 2 illustrates schematic diagrams of typical test apparatuses. The test apparatus consists of a superconducting magnet (SCM), a moving device, a specimen rod, a magnetic field sensor (hereafter  $H$  sensor), a magnetic dipole moment detection coil (hereafter  $M$  coil), measuring devices and a data processing device (PC). The measurement is carried out in an open magnetic circuit to enable the determination of magnetic properties of permanent magnet materials with coercivity higher than 2 MA/m.

The axis of the DC magnetic field generated by the SCM is vertical and coaxial with the  $M$  coil and the specimen rod. The moving test specimen is placed in a zone where the magnetic field strength is uniform with a tolerance of  $\pm 1\%$  at the centre of the SCM. The  $H$  sensor is placed in a zone where the influence of the magnetic dipole moment of the test specimen can be ignored.

A test specimen is firmly attached on the specimen rod so that the direction of magnetization is parallel to the axis of the specimen rod, and then placed in the test apparatus as shown in Figure 2.

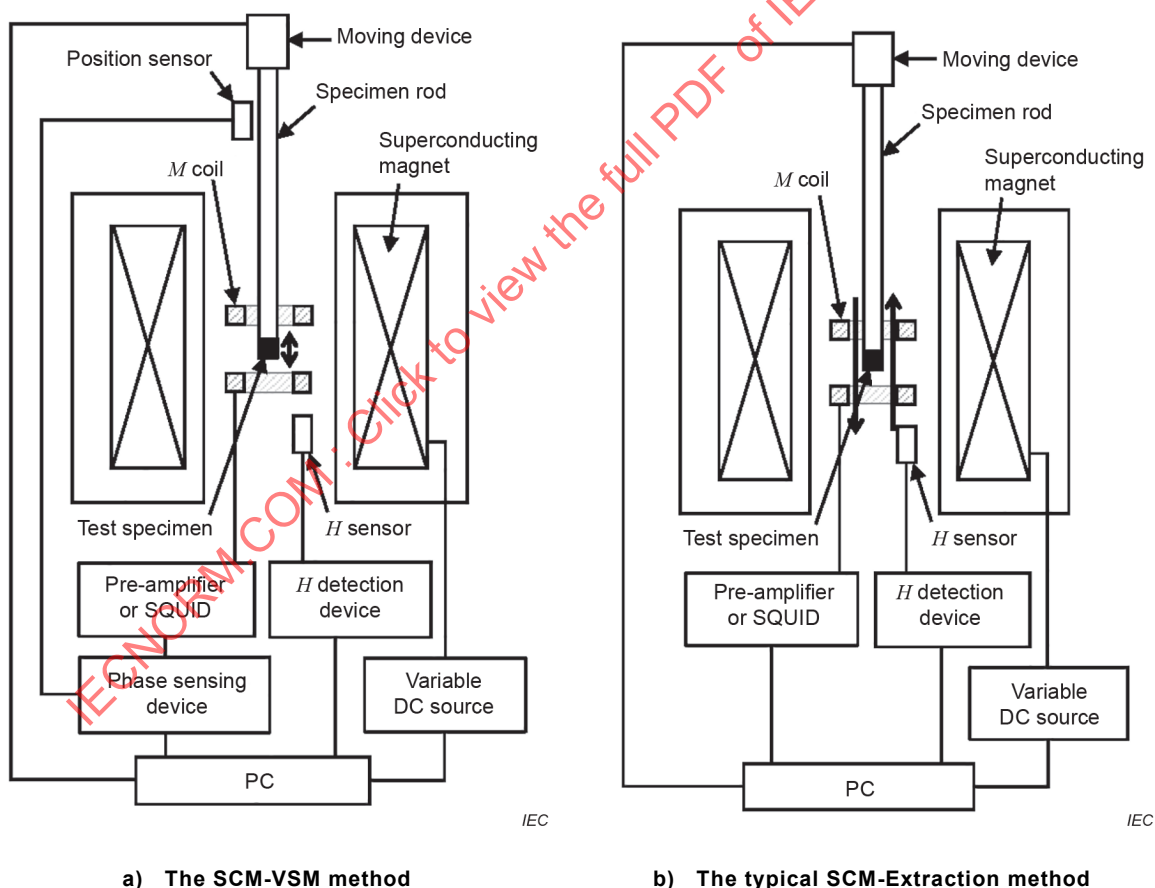


Figure 2 – Schematic diagrams of the test apparatus

The test specimen is initially magnetized to saturation (see 6.2), and then a DC magnetic field is applied to the test specimen in the direction opposite to that used for the initial magnetization. The magnetic field strength is measured by the  $H$  sensor (see 4.3).

The magnetic dipole moment of the test specimen is detected by the voltage induced in the  $M$  coil due to the movement of the test specimen (see 4.4). The magnetic polarization of the test specimen is calculated from the magnetic dipole moment and the volume of the test specimen (see 7.2). For calibration aspects, see Clause 9.

There are two methods different in modes of the movement of the test specimen:

- a) the SCM-VSM method: the test specimen is vibrated with a small amplitude in the  $M$  coil;
- b) the SCM-Extraction method: the test specimen is extracted through the  $M$  coil.

NOTE There is another method to determine the magnetic polarization of the test specimen, i.e. the SCM-Magnetometer method. In this method, variation of the magnetic polarization of the stationary test specimen due to variation of the magnetic field strength applied to the stationary test specimen is detected by the voltage induced in the detection coil ( $J$  coil) (see Annex A).

The measurements are carried out at an ambient temperature of  $(23 \pm 5) ^\circ\text{C}$ . For permanent magnet materials which are known to have significant temperature coefficients  $\alpha(J_r)$  and  $\alpha(H_{cJ})$ , the temperature of the test specimen should be in a range between  $19 ^\circ\text{C}$  and  $27 ^\circ\text{C}$  and controlled within a tolerance of  $\pm 1 ^\circ\text{C}$  during the measurements in accordance with IEC 60404-5. The temperature of the test specimen should be measured by a non-magnetic temperature sensor.

The demagnetization curve measured in an open magnetic circuit is influenced strongly by the self-demagnetizing field in the test specimen which opposes magnetization.

In order to determine the intrinsic demagnetization curve of the permanent magnet material, a correction of the influence of the self-demagnetizing field (hereafter demagnetizing field correction) should be applied to the measured demagnetization curve (see Clause 11). Magnetic properties of the permanent magnet material are determined from the corrected demagnetization curve.

These two methods have the following features:

- 1) The most important feature is that it is possible to determine all the magnetic properties of permanent magnet materials with coercivity higher than  $2 \text{ MA/m}$  in contrast to the method of measurement in a closed magnetic circuit in accordance with IEC 60404-5.
- 2) The reproducibility of measurement by the methods is comparable with that of IEC 60404-5. It was confirmed by the international round robin test (see Annex F).
- 3) The influence of eddy currents in the test specimen is negligible.
- 4) By adopting the ceramic SCM made of ceramic high temperature superconducting coil, demagnetization curve can be measured within several minutes without using expensive liquid helium and its incidental facilities (see Annex C). Also test apparatus using the ceramic SCM which can deal test specimens of industrial size has been commercialized for industrial use. So, it is convenient for industrial use globally.
- 5) There is no drift in the signal of the magnetic dipole moment, owing to the use of a phase sensing device (lock-in amplifier) in the SCM-VSM.

#### 4.2 Superconducting magnet (SCM)

A variable DC source supplies a DC current to the superconducting coil, with sufficiently low voltage noise (see Figure 2). The current source should be a bipolar type which can switch positive-negative polarity continuously.

The SCM is recommended to have a capacity to generate a magnetic field strength more than  $4,8 \text{ MA/m}$  ( $6 \text{ T}$  in magnetic flux density) in order to measure the magnetic properties of permanent magnet materials with coercivity higher than  $2 \text{ MA/m}$ , e.g. Nd-Fe-B sintered magnets.

It is recommended to adopt the ceramic SCM made of ceramic high temperature superconducting coil rather than a conventional metallic SCM made of metallic superconducting coil, in order to reduce the time required to measure a demagnetization curve within several minutes. It is particularly convenient for industrial use (see Annex C).

The zone of uniform magnetic field strength generated at the centre of the SCM should be sufficiently large to include the space of the moving test specimen.

#### 4.3 Magnetic field strength sensor ( $H$ sensor)

An  $H$  sensor such as a Hall probe is used to measure the magnetic field strength together with a suitable  $H$  detection device (see Figure 2). The  $H$  sensor should be calibrated by an appropriate method such as Nuclear Magnetic Resonance (NMR).

In the case of a calibrated SCM, the magnetic field strength may be measured from the magnetizing current supplied to the SCM. Care should be taken if there is a small hysteresis between the magnetizing current and the magnetic field strength of the SCM.

The total measuring error of the magnetic field strength should be smaller than  $\pm 1\%$ .

#### 4.4 Magnetic dipole moment detection coil ( $M$ coil)

The magnetic dipole moment of the test specimen is measured by the voltage induced in the  $M$  coil placed near the test specimen (see Figure 2). The  $M$  coil is wound coaxially with the axis of magnetic field and placed symmetrically with respect to the centre of the magnetic field. Electrical leads of the  $M$  coil should be tightly twisted to avoid errors caused by voltages induced in loops of the leads.

The voltage induced in the  $M$  coil should be calibrated using a standard specimen of nickel sphere and the influence of the shape and dimensions of the test specimen on the voltage should be verified (see Clause 9).

The total measuring error of the magnetic dipole moment should be smaller than  $\pm 1\%$ .

The  $M$  coil used in this document is the first order gradiometer coil which is composed of an upper coil and a lower coil connected electrically in opposite polarity as shown in Figure 3. The second order gradiometer coil combined with a SQUID (superconducting quantum interference device) circuit can also be used for the  $M$  coil (see Annex D).

NOTE Figure D.2 illustrates the dependence of the induced voltage on the position of the test specimen in the SCM-Extraction method.

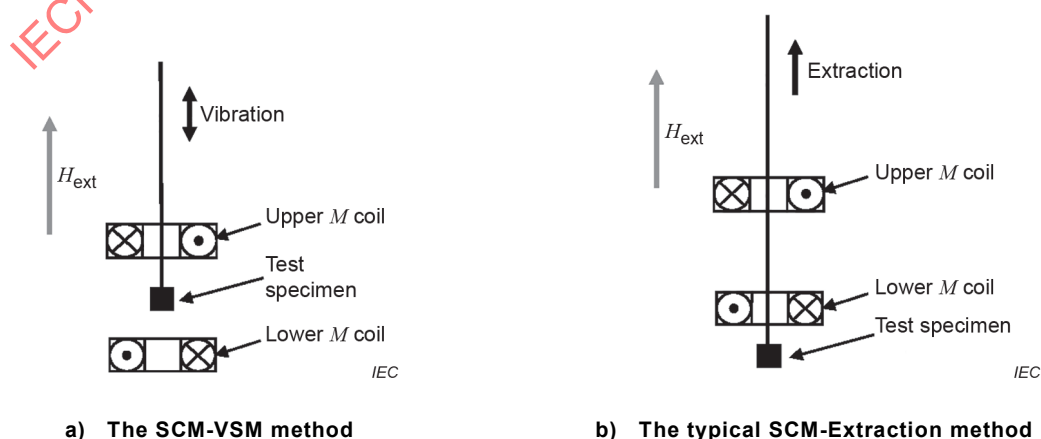


Figure 3 – Schematic diagrams of the first order gradiometer coil

#### 4.5 Specimen rod and moving device

The test specimen should be attached firmly at the bottom end of the specimen rod to avoid unexpected movement of the test specimen in the magnetic field. Then the specimen rod is inserted vertically in the SCM and connected to the moving device at the top end as shown in Figure 2.

The specimen rod should be non-magnetic and should have high rigidity to keep the test specimen on the axis of the magnetic field without trembling.

The moving device can be a linear motor, a voice coil or other system which can move or vibrate the specimen rod linearly along the axis of the magnetic field.

Moving modes of the test specimen are as follows.

a) the SCM-VSM method

The test specimen is vibrated at a fixed frequency and amplitude sufficiently smaller than the length of the  $M$  coil. The frequency is normally 20 Hz to 200 Hz and the amplitude is typically from 0,5 mm to 2 mm [see Figure 3 a)].

b) the SCM-Extraction method

The test specimen is extracted along the axis of the magnetic field. The start point of the moving specimen is below the lower  $M$  coil or above the upper  $M$  coil [see Figure 3 b)].

#### 4.6 Measuring devices and the data processing device

The voltage induced in the calibrated  $M$  coil due to the movement of the test specimen is proportional to the magnetic dipole moment of the test specimen. The signal of the  $M$  coil is fed to a preamplifier. In the case of the second order gradiometer coil, a SQUID circuit is employed to integrate the signal (see Figure 2).

In the SCM-VSM method, the amplified signal is fed to a phase sensing device such as a lock-in amplifier to output the amplitude of the signal synchronized to the vibration frequency of the test specimen. The output signal is fed to the data processing device.

In the SCM-Extraction method, the amplified signal is directly fed to the data processing device.

The output signal of the magnetic field detecting device, which is proportional to the magnetic field strength, is fed to the data processing device.

The data processing device is usually composed of a digitizer and a digital signal calculator for the determination of the magnetic properties. The digitizer converts the input signals into digital data simultaneously with analogue-to-digital converters (ADC). The ADC should have at least a 16-bit resolution.

The digital signal calculator is usually a personal computer (PC) and calculates the magnetic properties from the digitized signals of the magnetic dipole moment and the magnetic field strength.

### 5 Test specimen

The shape of the test specimen is cylinder or cuboid.

The ratio of the length  $L$  to the dimension  $D$  i.e.  $L/D$  is 1,00 within  $\pm 0,05$ , where  $D$  is the edge length of the cuboid test specimen or the diameter of the cylinder test specimen. In the case of cuboid with  $L/D = 1,00$ , care should be taken that the direction of magnetization is marked properly during the test specimen preparation. The direction of magnetization is parallel to the length  $L$  of the specimen.

NOTE A small difference between  $L$  and  $D$  of a cuboid test specimen is convenient to easily identify the magnetizing direction of the test specimen.

The dimension of the test specimen, i.e.  $L$  and  $D$ , is equal to or larger than 3 mm but sufficiently smaller than that of the  $M$  coil (see Annex B).

The test specimen should be cut carefully to the predetermined dimension from a large block of the permanent magnet material. Care should be taken to avoid damage on its surface which can deteriorate the magnetic properties.

Test specimens with a dimension less than 3 mm can be used, provided that the damaged surface layer is negligible or a special treatment is applied on the damaged surface layer to recover the intrinsic magnetic properties.

The test specimen should be marked with an arrow to indicate the direction of magnetization in order to make it easy to attach the test specimen to the specimen rod.

## 6 Preparation of measurement

### 6.1 Measurement of volume of the test specimen

The volume  $V$  of the test specimen should be calculated from the mass and the density of the test specimen. The mass of the test specimen can be determined accurately by means of an electronic balance. The density of the test specimen can be determined accurately with a large block of the permanent magnet material.

The volume  $V$  can also be calculated from the dimensions of the test specimen measured by means of a calibrated micrometre with four significant figures.

The volume  $V$  of the test specimen should be determined within a tolerance of  $\pm 1$  %.

### 6.2 Initial magnetization of the test specimen to saturation

Before measurement, the test specimen is magnetized to saturation in a DC magnetic field strength  $H_{\text{mag}}$ .

If it is not possible to magnetize the test specimen to saturation in the test apparatus, the test specimen should be magnetized to saturation outside the test apparatus in a superconducting coil or a pulse magnetizer in accordance with IEC 60404-5.

Recommended values for the DC magnetic field strength  $H_{\text{mag}}$  for various permanent magnet materials can be found in IEC TR 62517 [2].

## 7 Determination of magnetic polarization

### 7.1 Measurement of the magnetic dipole moment

In the SCM-VSM method, the test specimen is vibrated at a fixed frequency and amplitude, and then the output voltage of the phase sensing device is measured (see 4.6).

The magnetic dipole moment  $m$  is calculated from Formula (1):

$$m = \frac{C_v U_v}{a \cdot f} \quad (1)$$

where

$m$  is the magnetic dipole moment, in  $\text{Wb} \cdot \text{m}$ ;

$U_v$  is the output voltage of the phase sensing device, in V;

$C_v$  is a constant, in  $\text{m}^2$ ;

$a$  is the amplitude of the vibration, in m;

$f$  is the frequency of the vibration, in Hz.

In the SCM-Extraction method, the test specimen is extracted through the  $M$  coil. The output voltage of the pre-amplifier or the SQUID circuit is measured (see 4.6).

The magnetic dipole moment is calculated from Formula (2):

$$m = C_1 \int_{t_1}^{t_2} U(t) dt \quad (2)$$

where

$m$  is the magnetic dipole moment, in  $\text{Wb} \cdot \text{m}$ ;

$U(t)$  is the output voltage of the pre-amplifier or the SQUID circuit, in V;

$t_1$  is the time when the test specimen goes through the lower part of the  $M$  coil and  $U(t_1) = 0$ , in s;

$t_2$  is the time when the test specimen goes through the upper part of the  $M$  coil and  $U(t_2) = 0$ , in s;

$C_1$  is a constant, in m.

The constants  $C_v$  and  $C_1$  should be determined by a calibration of the  $M$  coil (see Clause 9).

## 7.2 Determination of magnetic polarization

The magnetic polarization  $J$  is calculated from the magnetic dipole moment  $m$  and the volume of the test specimen  $V$  according to Formula (3).

$$J = \frac{m}{V} \quad (3)$$

where

$J$  is the magnetic polarization, in T;

$m$  is the magnetic dipole moment, in  $\text{Wb} \cdot \text{m}$ ;

$V$  is the volume of the test specimen, in  $\text{m}^3$ .

## 8 Measurement of magnetic field

The magnetic field strength  $H$  corresponding to the magnetic polarization is measured by the calibrated  $H$  sensor, e.g. a Hall probe, and the  $H$  detection device (see Figure 2).

The temperature dependence of the measuring instrument is to be taken into account.

## 9 Calibration of the magnetic dipole moment detection coil ( $M$ coil)

The calibration of the  $M$  coil should be carried out by measuring a standard specimen of nickel sphere for which the magnetic dipole moment  $m$  at an ambient temperature of  $(23 \pm 5) ^\circ\text{C}$  and an applied magnetic field strength of 398 kA/m (5 kOe) is certificated by a national or accredited calibration laboratory with the temperature coefficient [3]. The standard specimen should be made of 99,9 % or higher purity nickel and stress-relief annealed without oxidation. The space occupied by the standard specimen including its movement during the measurement should be sufficiently smaller than the uniform field region of the SCM coil. Then, the magnetic field generated by the standard specimen is a perfect dipole field and identical to the field generated by an ideal dipole in the centre of the spherical standard specimen.

NOTE A saturation magnetic moment is not suitable for calibration in this document.

The constant  $C_v$  of Formula (1) or  $C_1$  of Formula (2) is determined so that the measured magnetic dipole moment at magnetic field strength of 398 kA/m (5 kOe) matches with the certificated value of magnetic dipole moment of the nickel sphere. The difference between the ambient temperatures at the calibration and that specified in the certification should be compensated by using the temperature coefficient specified in the certification.

The shape and dimension dependence of the measured magnetic dipole moment of the test specimen should be verified and compensated. The verification should be carried out by comparison of measurements using a nickel sphere with the same dimension as the standard specimen and a nickel cube or cylinder with the same shape and dimensions as the test specimen. The nickel sphere and the nickel cube or cylinder should be made of the same material of 99,9 % or higher purity nickel and stress-relief annealed without oxidation.

## 10 Determination of demagnetization curve

The demagnetization curve is a part of the hysteresis loop  $J(H)$  (see Figure 1).

The measurement procedure of the demagnetization curve is as follows.

At first, the test specimen, which is initially magnetized to saturation, is placed in the homogeneous magnetic field as shown in Figure 2. The position of the test specimen is adjusted vertically and horizontally at the centre of the  $M$  coil.

The magnetizing current supplied to the SCM is increased to magnetize the test specimen to saturation.

Then the magnetizing current is reduced to zero to reach zero external magnetic field strength. Then the magnetizing current is turned to the reverse direction and increased until the magnetic field strength has passed the coercivity  $H_{cJ}$ .

The speed of variation of the magnetic field strength is sufficiently slow in accordance with IEC 60404-5 to avoid significant magnetic viscosity and eddy currents which can affect the measured value.

The magnetic dipole moment of the test specimen is measured by vibrating the test specimen (SCM-VSM method) or by extracting the test specimen (SCM-Extraction method) (see 7.1). The corresponding magnetic field strength is measured.

The demagnetization curve is obtained either from a continuous measurement with changing the magnetic field strength or from point-by-point measurements at discrete magnetic field strength.

The value of magnetic polarization is determined from the measured value of the magnetic dipole moment (see 7.2), and then the demagnetization curve  $J(H)$  is drawn relating values of the magnetic polarization to the corresponding values of the magnetic field strength.

The measured demagnetization curve is influenced strongly by the self-demagnetizing field in the test specimen. Therefore, in order to determine the intrinsic demagnetization curve and the principal magnetic properties, the demagnetizing field correction should be applied on the measured demagnetization curve.

## 11 Demagnetizing field correction

### 11.1 General

Figure 4 illustrates the relationship between the magnetic polarization  $\vec{J}$  and the self-demagnetizing field  $\vec{H}_d$ . When a block of a permanent magnet material is magnetized in an external magnetic field  $\vec{H}_{ext}$ , magnetic poles are generated on the ends of the block in the direction of the external magnetic field, simultaneously with the magnetic polarization  $\vec{J}$  in the block.

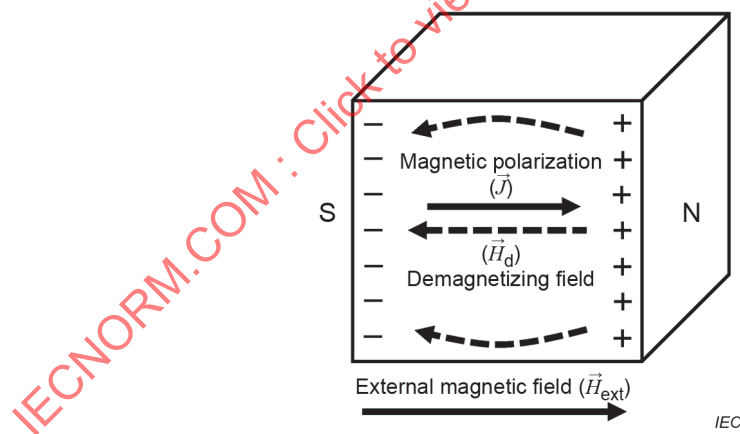


**Figure 4 – Relationship between magnetic polarization and self-demagnetizing field**

NOTE 1 The demagnetizing field is uniform only in case of ellipsoidal form of the test specimen. As can be seen from Figure 4 the demagnetization field of the cube test specimen is not uniform. That is why it is difficult to evaluate the real value of  $\vec{H}_d$  and several methods are proposed.

A self-demagnetizing field  $\vec{H}_d$  is generated by the magnetic poles in the block opposite to the direction of the external magnetic field  $\vec{H}_{ext}$ . The self-demagnetizing field  $\vec{H}_d$  increases proportionally with the magnetic polarization  $J$ . The effective magnetic field  $\vec{H}_{eff}$  acting on the magnetization of the permanent magnet material is expressed by Formula (4).

$$\vec{H}_{\text{eff}} = \vec{H}_{\text{ext}} + \vec{H}_{\text{d}} \quad (4)$$

where

$\vec{H}_{\text{eff}}$  is the effective magnetic field, in A/m;

$\vec{H}_{\text{ext}}$  is the external magnetic field, in A/m;

$\vec{H}_{\text{d}}$  is the demagnetizing magnetic field, in A/m.

Figure 5 illustrates a schematic diagram of the demagnetizing field correction. The demagnetizing field correction converts the measured demagnetization curve  $J(H_{\text{ext}})$  into the intrinsic demagnetization curve  $J(H_{\text{eff}})$ .

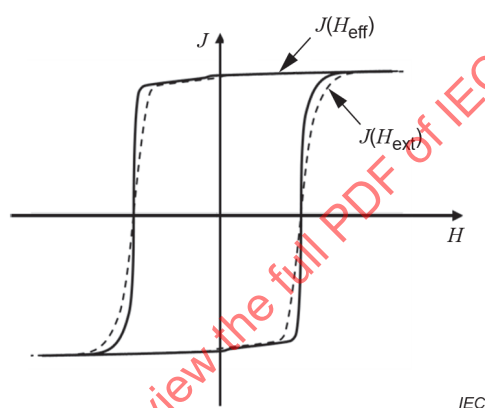


**Figure 5 – Schematic diagram of the demagnetizing field correction**

There are three methods of the demagnetizing field correction:

- Method A: the method using a demagnetizing factor determined by the shape of the test specimen only;
- Method B: the method using a demagnetizing factor determined by the shape and the magnetic susceptibility of the test specimen;
- Method C: the method using an inverse analysis considering the spatial distribution of the self-demagnetizing field strength in the test specimen.

NOTE 2 In the case of an open magnetic circuit, the self-demagnetizing field generated in the test specimen is generally distributed spatially. In the case that an accurate squareness of the demagnetization curve is needed, Method C is preferable for high accuracy of squareness evaluation since this method simulates the actual distribution of the self-demagnetizing field strength.

Table 1 compares features of the above demagnetizing field correction methods for correction accuracy and calculation time. The correction accuracy is evaluated as the difference between the corrected demagnetization curve and the demagnetization curve measured by means of a permeameter in accordance with IEC 60404-5.

**Table 1 – Features of the demagnetizing field correction methods in comparison with Method B**

	Method A	Method B	Method C
Correction accuracy	not high	(reference)	sufficiently high
Calculation time	shorter	(reference)	longer

NOTE 3 These methods are applicable to the demagnetization curve measured in an open magnetic circuit. In the pulsed field magnetometer (PFM) method, corrections of the eddy currents in the magnet and the magnetic viscosity of the permanent magnet material are applied to the measured demagnetization curve in addition to the demagnetizing field correction (See IEC TR 62331:2005, 7.1.6. [1]).

**11.2 Method A: Method using a demagnetizing factor determined by the shape of the test specimen only**

Method A assumes that the self-demagnetizing field strength in the test specimen is uniform and determined by the shape of the test specimen only. The strength of the self-demagnetizing field is calculated from Formula (5).

$$H_d = -N \frac{J}{\mu_0} \tag{5}$$

where

$H_d$  is the strength of the self-demagnetizing field, in A/m;

$N$  is the demagnetizing factor;

$J$  is the magnetic polarization, in T;

$\mu_0$  is the magnetic constant, in H/m;  $\mu_0 \cong 4 \pi \times 10^{-7}$ .

The demagnetizing factor  $N$  is calculated from the permeance coefficient  $P_c$  of the permanent magnet material, which is determined according to the shape of the test specimen [4], [5].

The measured demagnetization curve  $J(H_{ext})$  is converted to the demagnetization curve  $J(H_{eff})$  using Formulas (4) and (5).

NOTE There is a spatial distribution of the self-demagnetizing field strength in actual magnets except for the case that the shape of the test specimen is ellipsoidal. However, Method A assumes the self-demagnetizing field strength in the test specimen is uniform independent of the shape. Hence the accuracy of this method is not high.

**11.3 Method B: Method using a demagnetizing factor determined by the shape and the magnetic susceptibility of the test specimen**

Method B calculates the demagnetizing factor  $N$  of the test specimen using a finite element method (FEM) with respect to the shape and the magnetic susceptibility  $\chi$  of the test specimen.

The demagnetizing factor  $N$  corresponding to the shape and magnetic susceptibility  $\chi$  of the test specimen can be found in literature (see Table 1 in [6]).

The measured demagnetization curve  $J(H_{ext})$  is converted to the demagnetization curve  $J(H_{eff})$  using the above demagnetizing factor  $N$  and Formulas (4) and (5).

NOTE Method B assumes the self-demagnetizing field strength in the test specimen is not uniform, and is dependent on the shape and the magnetic susceptibility  $\chi$ . Hence the accuracy is improved, but not high enough.

#### 11.4 Method C: Method using an inverse analysis considering the spatial distribution of the self-demagnetizing field strength in the test specimen

Method C initially assumes a temporary hysteresis loop  $J(H)$  and then modifies it so that the calculated demagnetization curve coincides with the measured hysteresis loop  $J(H_{\text{ext}})$ . This method executes an inverse analysis considering the spatial distribution of the self-demagnetizing field strength in the test specimen using a FEM [7].

Method C does not use the demagnetizing factor  $N$  to correct the measured demagnetization curve  $J(H_{\text{ext}})$ .

This method assumes the temporary hysteresis loop  $J(H)$  as defined in Formula (6). The parameter  $\alpha(H)$  is corrected in iterations of calculation so that the assumed hysteresis loop  $J(H)$  influenced by the self-demagnetizing field strength  $H_d$  coincides with the measured hysteresis loop  $J(H_{\text{ext}})$ .

$$J(H) = \gamma \tanh\left(\frac{H - \beta}{1 - \alpha(H)}\right) + (H - \beta)(1 + 0,1\alpha(H)) \quad (6)$$

where

- $J$  is the magnetic polarization, in T;
- $H$  is the magnetic field strength, in A/m;
- $\alpha(H)$  is a parameter as a function of  $H$ ;
- $\beta$  and  $\gamma$  are parameters.

Figure 6 illustrates a conceptual diagram of the procedure of this method. Based on the assumed hysteresis loop  $J(H)$  defined in Formula (6), the distribution of the self-demagnetizing field strength and local hysteresis loops  $J(H)$  in cells of the magnet model is calculated using a FEM. Then, parameters  $\alpha(H)$ ,  $\beta$  and  $\gamma$  in Formula (6) are modified by comparing the calculated hysteresis loop  $J(H_{\text{eff}})$  and the measured hysteresis loop  $J(H_{\text{ext}})$ .

Such operations are repeated until the difference between those hysteresis loops becomes smaller than 5 %. If this condition is satisfied, the calculated hysteresis loop  $J(H_{\text{eff}})$  can be considered as the corrected demagnetization curve. For the detailed algorithm, see Annex E.

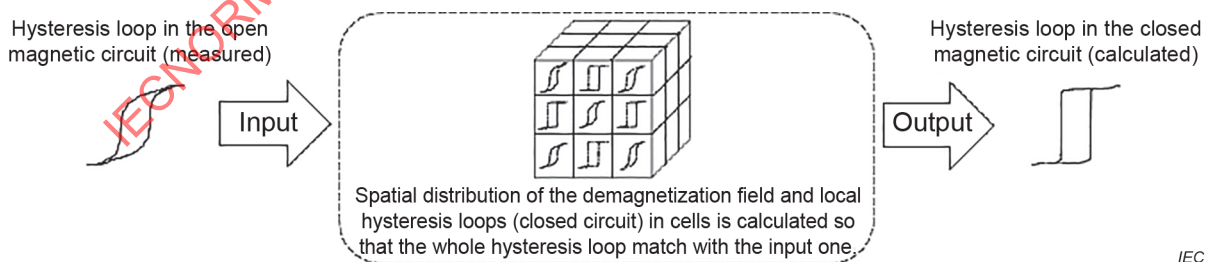


Figure 6 – Conceptual diagram of the procedure of Method C

## 12 Determination of principal magnetic properties

### 12.1 Remanent magnetic polarization $J_r$

The remanent magnetic polarization  $J_r$  is given by the intercept of the corrected demagnetization curve  $J(H_{\text{eff}})$  with the  $J$  axis ( $H_{\text{eff}} = 0$ ).

NOTE The remanent magnetic polarization has the same value as the remanent flux density.

### 12.2 Maximum energy product $(BH)_{\max}$

The maximum energy product  $(BH)_{\max}$  is the maximum value of the modulus of the product of corresponding values of  $B$  and  $H_{\text{eff}}$  on the demagnetization curve  $B(H_{\text{eff}})$ .

The demagnetization curve  $B(H_{\text{eff}})$  is calculated from Formula (7) using the corrected demagnetization curve  $J(H_{\text{eff}})$ .

$$B = J + \mu_0 H_{\text{eff}} \quad (7)$$

where

$B$  is the magnetic flux density, in T;

$J$  is the magnetic polarization, in T;

$\mu_0$  is the magnetic constant, in H/m;  $\mu_0 \cong 4 \pi \times 10^{-7}$ ;

$H_{\text{eff}}$  is the effective magnetic field strength, in A/m.

### 12.3 Coercivity ( $H_{cJ}$ and $H_{cB}$ )

The coercivity  $H_{cJ}$  is given by the intercept of the corrected demagnetization curve  $J(H_{\text{eff}})$  with the  $H$  axis ( $J = 0$ ).

The coercivity  $H_{cB}$  is given by the intercept of the demagnetization curve  $B(H_{\text{eff}})$  with the  $H$  axis ( $B = 0$ ).

## 13 Reproducibility

The reproducibility of the measurements described in this document is characterized by a relative standard deviation given in Table 2 based on the results of the international round robin test (see Annex F).

**Table 2 – Reproducibility of the magnetic properties**

	Relative standard deviation
$J_r$	1 %
$H_{cJ}$	1 %
$(BH)_{\max}$	1,5 %

NOTE The reproducibility of the measurements can be comparable with that of IEC 60404-5. The magnetic dipole moment of the test specimen is measured instead of the magnetic flux through the detection coil ( $J$  coil), and there is no measurement error caused by non-uniform air gaps between the test specimen and the pole pieces.

## 14 Test report

The test report contains the following, as applicable:

- a) the type and condition of the test specimen;

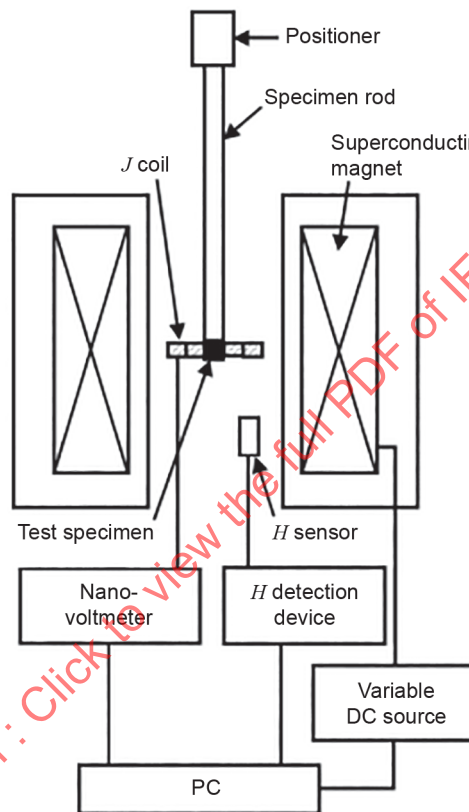
- b) the shape, dimension and volume of the test specimen;
- c) the temperature of the test specimen during measurement;
- d) the method of initial magnetization to saturation;
- e) the measuring method of the magnetic dipole moment;
- f) the type of magnetic dipole moment detection coil ( $M$  coil);
- g) the speed of variation of the magnetic field strength during the measurement;
- h) the method of demagnetizing field correction;
- i) the measured demagnetization curve;
- j) the corrected demagnetization curve;
- k) the saturation magnetic polarization  $J_s$ ;
- l) the remanent magnetic polarization  $J_r$ ;
- m) the coercivity ( $H_{cJ}$  and  $H_{cB}$ );
- n) the maximum energy product  $(BH)_{\max}$ ;
- o) the values of  $B$  and  $H$  for  $(BH)_{\max}$ ;
- p) in the case of anisotropic material: the angle of magnetization with respect to the preferred axis of the material if this angle differs from zero degrees;
- q) the estimated uncertainty of the measurement.

IECNORM.COM : Click to view the full PDF of IEC TR 63304:2021

## Annex A (informative)

### SCM-Magnetometer method

Figure A.1 illustrates the schematic diagram of a typical test apparatus of the SCM-Magnetometer method [8]. The test apparatus consists of a superconducting magnet, a positioner, a specimen rod, a magnetic field sensor ( $H$  sensor), a magnetic polarization detection coil ( $J$  coil), measuring devices and a data processing device (PC). The measurement is carried out in an open magnetic circuit to enable to determine magnetic properties of permanent magnet materials with coercivity higher than 2 MA/m.



IEC

**Figure A.1 – Schematic diagram of the test apparatus  
for the SCM-Magnetometer method**

This method is different from the SCM-VSM and SCM-Extraction methods in the type of detection coil and keeping the test specimen stationary. The detection coil and the stationary test specimen are similar to the method of measurement in a closed magnetic circuit in accordance with IEC 60404-5 (see Figure A.2).

The ceramic SCM made of ceramic superconducting coil should be used. The conventional metallic SCM made of metallic superconducting coil is not suitable for this method, because the speed of variation of the magnetic field is too slow to achieve enough sensitivity to measure the magnetic polarization (see Annex C).

The detection coil is a concentric search coil (hereafter  $J$  coil), which is composed of an inner detection coil and an outer field compensation coil connected electrically in opposition to compensate air flux. Since the voltage induced in the  $J$  coil is extremely weak due to the lower speed of variation of the magnetic field in this method, the number of the coil turns is usually more than 1 000. The signal of the  $J$  coil is fed to a nanovoltmeter and amplified. The amplified signal is fed to the data processing device and integrated numerically. For details of the data processing device, see 4.6.

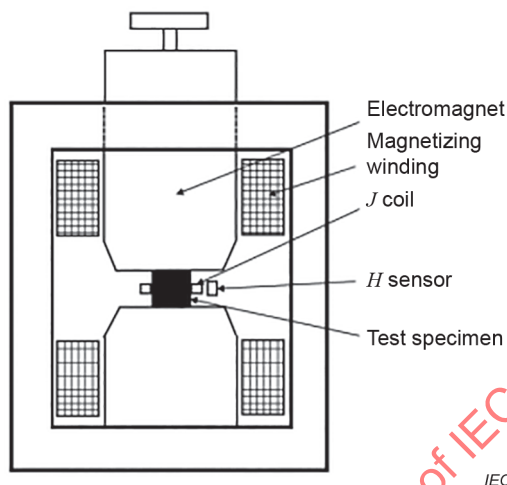


**Figure A.2 – Schematic diagrams of the test apparatus for the method in a closed magnetic circuit in accordance with IEC 60404-5**

The  $J$  coil detects the magnetic polarization of the test specimen which is inserted into the  $J$  coil (see Figure A.1). The voltage induced in the  $J$  coil is proportional to the time derivative of the magnetic polarization of the test specimen. The magnetic polarization  $J$  is determined by the integration of the voltage induced in the  $J$  coil caused by the applied magnetic field.

The voltage  $U$  induced in the  $J$  coil is given by Formula (A.1).

$$U = (N_A - N_B) S_s \frac{dJ}{dt} \quad (\text{A.1})$$

where

$U$  is the voltage induced in the  $J$  coil, in V;

$N_A$  is the number of turns on the inner detection coil;

$N_B$  is the number of turns on the outer field compensation coil;

$S_s$  is the cross-sectional area of the test specimen, in  $\text{m}^2$ .

The magnetic polarization  $J$  is given by Formula (A.2).

$$J = -\frac{1}{(N_A - N_B) S_s} \int U dt \quad (\text{A.2})$$

In this method, a correction of drift in the  $J$  signal, which is accompanied with the integration of weak signals, is indispensable.

## Annex B (informative)

### Effects of the test specimen dimensions

This Annex B describes the effects of the test specimen dimensions on the coercivity mechanism and the magnetic properties measurement of permanent magnets. It gives also dimension restrictions for the measuring test specimen.

The coercivity of SmCo<sub>5</sub> and Nd-Fe-B sintered magnets is dominated by the nucleation mechanism. For these materials, it is important to pay attention to the surface degradation of test specimens at preparation. The effect of the surface degradation which appears on the demagnetization curves of Nd-Fe-B sintered magnets are precisely reported including the recovery procedure with grain boundary diffusion [9], [10], [11], [12].

Figure B.1 shows the effects of test specimen dimensions on measured magnetic properties [ $B_r$ ,  $H_{cJ}$ ,  $H_{cB}$  and  $(BH)_{max}$ ] for Nd-Fe-B sintered magnets with different coercivities. The test specimens are cubes with side lengths of 1,0 mm, 2,0 mm, 3,0 mm and 4,0 mm. The corresponding  $S/V$  values ( $S$ : surface area and  $V$ : volume of the test specimen) are  $6\text{ mm}^{-1}$ ,  $3\text{ mm}^{-1}$ ,  $2\text{ mm}^{-1}$  and  $1,5\text{ mm}^{-1}$ , respectively. Measurements of magnetic properties of bulk magnet materials without influence of the surface degradation are preferable. Therefore, lower  $S/V$  values are preferable. From Figure B.1 the test specimen of 3,0 mm cube can be used for evaluation of magnetic properties of the bulk magnet material. So,  $S/V$  values lower than  $2\text{ mm}^{-1}$  are required.

The VSM method has been used to evaluate magnetic properties of very small test specimens in the field of materials science. After development of high energy product Rare Earth (RE) magnets, very small magnets have been applied to optical pick-up devices, etc. Therefore, the evaluation of small magnets has been required in industry. Rigidity of the specimen rod restricts the larger dimensions of the test specimen in the VSM method. Recently a highly rigid specimen rod, which is capable to measure Nd-Fe-B sintered magnets of 10 mm in diameter and 14 mm in thickness, has been developed for the VSM method [13].

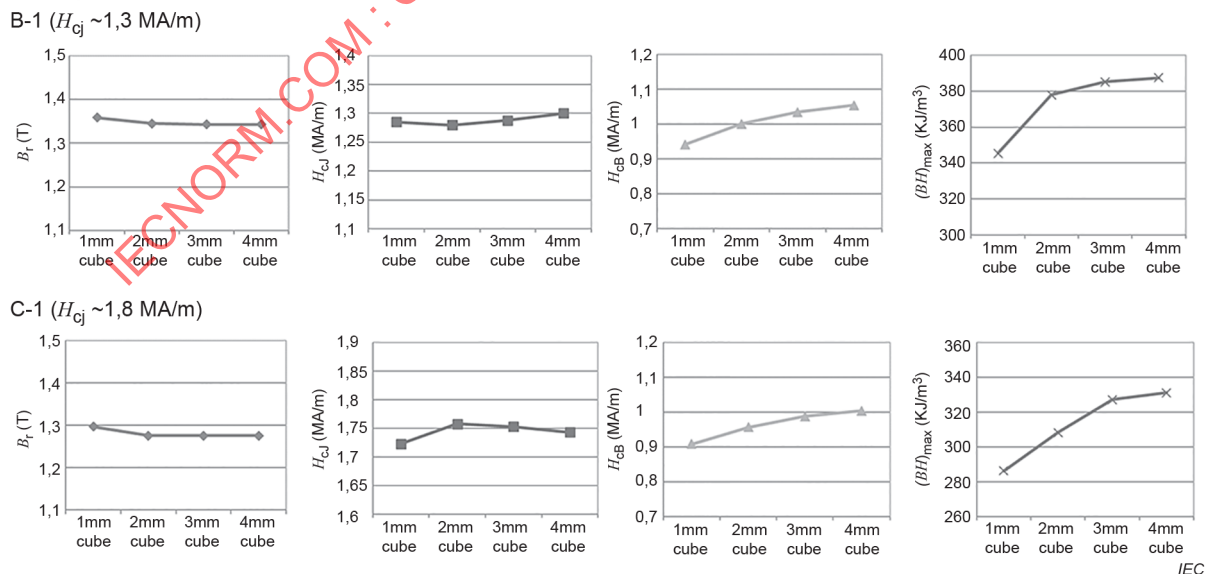


**Figure B.1 – Effects of test specimen dimensions on magnetic properties [ $B_r$ ,  $H_{cJ}$ ,  $H_{cB}$  and  $(BH)_{max}$ ] for Nd-Fe-B sintered magnets with different coercivities**

## Annex C (informative)

### Superconducting magnets (SCMs)

This Annex C describes two kinds of SCMs for the magnetic field generator, i.e. the conventional metallic SCM made of metallic superconducting coil and the newly developed ceramic SCM made of ceramic superconducting coil. The ceramic superconducting coil is also called a high temperature superconducting coil due to its high transition temperature from the normal state to the superconducting state. The metallic superconducting coil has a weak point that the speed of variation of magnetic field strength is limited in a low value to avoid a quench which destroys the superconducting state of the coil.

A Bi-based ceramic superconducting coil capable to be operated around 20 K cooled without using expensive liquid He has been developed. The heat capacity of the Bi-based superconducting coils is 0,13 MJ/m<sup>3</sup>K at 20 K which is 100 times higher than 0,001 4 MJ/m<sup>3</sup>K at 4 K of NbTi-based metallic superconducting coils [14], [15]. The higher heat capacity enables the higher speed of variation of magnetic field strength while avoiding a quench. The potential sweep rate of the Bi-based ceramic superconducting coil is 48 MA/m/min. The higher heat capacity prevents temperature increase caused by AC loss in the coil.

A comparison of the performance of the two SCMs is shown in Table C.1. The remarkable properties of the ceramic SCM is in the higher speed of variation of magnetic field strength, which is 20 times higher than the metallic SCM. It can take 3 min to measure a full hysteresis loop of a span of magnetic field strength of ±4,8 MA/m. It is comparable with that of the method of measurement in a closed magnetic circuit in accordance with IEC 60404-5.

**Table C.1 – Performance of SCMs**

	Metallic SCM	Ceramic SCM
Maximum Magnetic field strength (MA/m)	4,0 to 8,0	4,0 to 8,0
Typical speed of variation of magnetic field strength (MA/m/min)	0,42 (4,2 MA/m/10 min)	8,0 (4,0 MA/m/0,5 min)

Figure C.1 shows a typical structure of a ceramic SCM. The superconducting coil is composed of stacked pancake units in layers, thermally insulated from each other. The bore inserted in the superconducting coil is kept at room temperature.

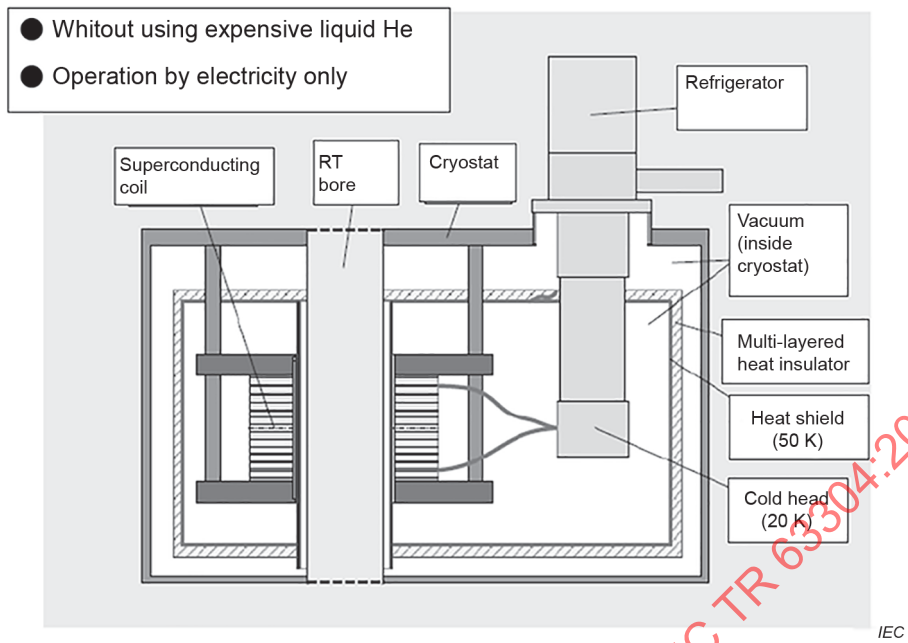


Figure C.1 – Typical cross-sectional structure of the ceramic SCM

IECNORM.COM : Click to view the full PDF of IEC TR 63304:2021

## Annex D (informative)

### Magnetic dipole moment detection coils ( $M$ coils)

This Annex D describes the magnetic dipole moment detection coils ( $M$  coils) for the SCM-VSM and the SCM-Extraction methods. The  $M$  coils used in these methods are the first order gradiometer coil which is composed of an upper coil and a lower coil connected electrically in opposite polarity as shown in Figure 3. The second order gradiometer coil as shown in Figure D.1 can be used with a SQUID circuit. The second order gradiometer coil and the SQUID circuit perform an integrator function as a magnetometer. The response of the SQUID circuit corresponding voltage induced in the second order gradiometer coil due to the movement of the test specimen is proportional to the magnetic dipole moment of the test specimen. The induced voltage in the gradiometer coils is not influenced by the external magnetic field.

The procedures of these SCM-methods are as follows.

#### a) The SCM-VSM method

Schematic diagrams of the first order gradiometer coil or the second order gradiometer coil in this method are illustrated in Figure 3 (a) and Figure D.1 [16], [17], [18], respectively. The vibrating direction of the test specimen is parallel to the magnetic field direction. This type of VSM was reported by A. Zieba and S. Foner in 1982 [19]. The dimension of the test specimen is smaller than the dimension of the  $M$  coil. The right position of the test specimen is determined by observing the output of the gradiometer coil due to change of position [16].

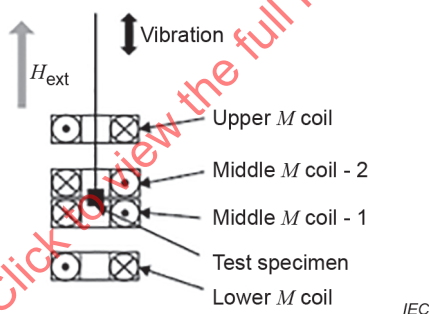


**Figure D.1 – Schematic diagram of the second order gradiometer coil for the SCM-VSM method**

#### b) The SCM-Extraction method

A schematic diagram of the first order gradiometer coil is illustrated in Figure 3 (b). The dependence of the induced voltage on the position of the specimen is shown in Figure D.2 [20], [21]. The test specimen moves from a position below the lower  $M$  coil to a position above the upper  $M$  coil along the axis of the magnetic field. The signal proportional to the magnetic dipole moment is obtained by time integral of the induced voltage regardless of variations in the speed of movement. In the case of SQUID, the second order gradiometer coil is also employed.

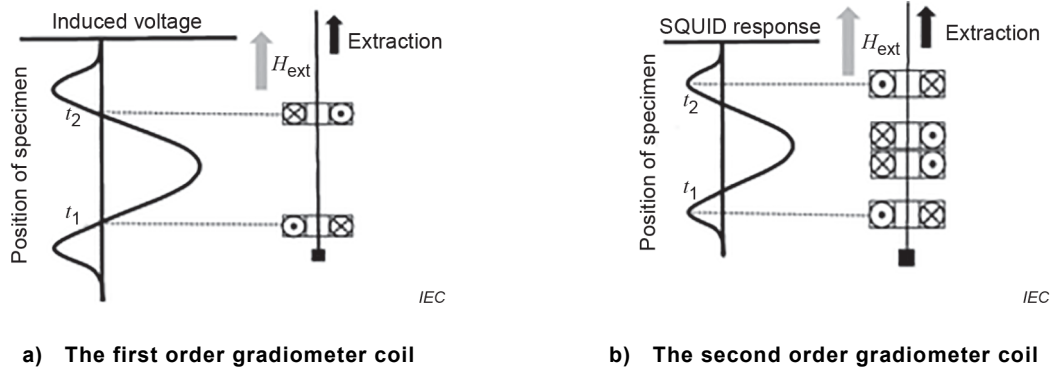


**Figure D.2 – Schematic diagram of the dependence of induced voltage on the position of the test specimen in the SCM-Extraction method**

IECNORM.COM : Click to view the full PDF of IEC TR 63304:2021

## Annex E (informative/normative)

### Details of the demagnetizing field correction

#### E.1 General

This Annex E describes details of Methods B and C of the demagnetizing field correction described in Clause 11.

#### E.2 Symbols

$J$	is the magnetic polarization, in T;
$\vec{J}$	is the magnetic polarization vector, in T;
$\chi$	is the magnetic susceptibility;
$\chi_{\text{ext}}$	is the measured magnetic susceptibility in an open magnetic circuit, $\chi_{\text{ext}} = J / H_{\text{ext}}$ ;
$H_{\text{eff}}$	is the strength of the effective magnetic field, in A/m;
$\vec{H}_{\text{ext}}$	is the external magnetic field vector, in A/m;
$H_{\text{ext}}$	is the strength of the external magnetic field applied to the magnet, in A/m;
$H_{\text{d}}$	is the strength of the self-demagnetizing field, in A/m;
$\vec{H}_{\text{d}}$	is the self-demagnetizing field vector, in A/m;
$N$	is the demagnetizing factor;
$N^{\text{S}}$	is the demagnetizing factor derived from the magnetic polarization;
$N^{\text{V}}$	is the demagnetizing factor derived from the strength of the self-demagnetizing field;
$\sigma$	is the magnetic charge density on the surface of the magnet, in Wb/m <sup>2</sup> ;
$\vec{e}^i$	is a unit normal vector on the surface of the magnet;
$\mu_0$	is the magnetic constant ( $4 \pi \times 10^{-7}$ ) in H/m;
$S'$	is the surface area of the magnet, in m <sup>2</sup> ;
$\hat{J}(x, y, z)$	is the spatial distribution of the magnetic polarization, in T;
$\hat{H}_{\text{d}}(x, y, z)$	is the spatial distribution of the self-demagnetizing field strength, in A/m;
$\hat{U}(x, y, z)$	is the magnetostatic potential, in A;
$J_{\text{open}}^{\text{exp}}(H)$	is the measured hysteresis loop in an open magnetic circuit, in T;
$J_{\text{open}}^{\text{sim}}(H)$	is the calculated hysteresis loop in an open magnetic circuit, in T;
$J_{\text{ideal}}(H)$	is the intrinsic hysteresis loop of the permanent magnet material, in T;
$J_{\text{r}}^{\text{exp}}$	is the remanent magnetic polarization extracted from the data in an open magnetic circuit, in T;
$H_{\text{C}}^{\text{exp}}$	is the coercivity extracted from the data in an open magnetic circuit, in A/m;
$H_{\text{max}}$	is the maximum external magnetic field extracted from the data in an open magnetic circuit, in A/m;

- $H_{\min}$  is the minimum external magnetic field extracted from the data in an open magnetic circuit, in A/m;
- $dJ_{\text{ave\_max}}$  is the maximum value of  $|J_{\text{open}}^{\text{exp}}(H_{\text{ext}}) - J_{\text{open}}^{\text{sim}}(H_{\text{ext}})|$  at all  $H_{\text{ext}}$ , in T;
- $\delta$  is the threshold in the convergence calculation of  $dJ_{\text{ave\_max}}$ , in T;
- $N(H_{\text{ext}})$  is the parameter of  $J_{\text{ideal}}(H)$ ;
- $dJ_{\text{err\_max}}$  is the maximum value of the residues of  $\hat{J}(x, y, z)$  in all meshes, in T;
- $\varepsilon$  is the threshold in the convergence calculation of  $dJ_{\text{err\_max}}$ , in T;
- $s$  is the constant value equal to 1, in m/A;
- $u$  is the constant value equal to 1, in 1/T.

**E.3 Method using a demagnetizing factor determined by the shape and magnetic susceptibility of the test specimen (Method B)**

The outline of the method proposed by Dr. Chen [6] is described as follows. The demagnetizing factor  $N$  in the z-direction of a cuboid magnet as illustrated in Figure E.1 is considered.

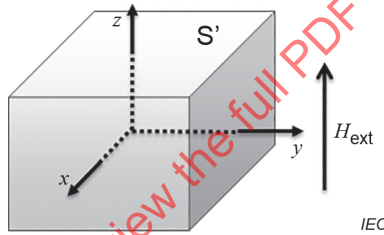


**Figure E.1 – Axes of a cuboid magnet**

The magnetic susceptibility  $\chi$  is defined as Formula (E.1).

$$\chi = \frac{J}{\mu_0 H_{\text{eff}}} \tag{E.1}$$

Assuming that the magnetic susceptibility  $\chi$  is uniform in the magnet and that the directions of the magnetic polarization  $J$ , the external magnetic field  $H_{\text{ext}}$  and the self-demagnetizing field  $H_d$  are parallel to the z-direction.

The relation between  $J$ ,  $H_{\text{ext}}$  and  $H_d$  is given as Formula (E.2).

$$J = \mu_0 \chi H_{\text{eff}} = \mu_0 \chi (H_{\text{ext}} + H_d) \tag{E.2}$$

The demagnetizing factor  $N$  is defined as Formula (E.3).

$$N \equiv -\frac{\mu_0 H_d}{J} \quad (\text{E.3})$$

The magnetic charge density on the surface of the magnet  $\sigma$  is expressed by Formula (E.4).

$$\sigma \equiv \vec{J} \cdot \vec{e} = \mu_0 \chi (\vec{H}_{\text{ext}} + \vec{H}_d) \cdot \vec{e} \quad (\text{E.4})$$

The strength of the self-demagnetizing field  $H_d$  due to the magnetic charge on the surface of the magnet is evaluated as Formula (E.5).

$$H_d = \frac{1}{4\pi\mu_0} \int_{S'} \frac{\sigma(r')(r-r')}{|r-r'|^3} dS' \quad (\text{E.5})$$

where

$r$  is the length from the origin, in m;

$r'$  is the coordinate variable, in m.

By using numerical discretization, Formulas (E.6) and (E.7) are derived,

$$\vec{H}_d = -\sum_{i,j=1}^n \bar{D}^{ij} \frac{\sigma^i}{\mu_0} \quad (\text{E.6})$$

$$\frac{\sigma^i}{\mu_0 \chi} + \sum_{j=1}^n \bar{e}^{-i} \cdot \bar{D}^{ij} \frac{\sigma^j}{\mu_0} = \bar{e}^{-i} \cdot \vec{H}_{\text{ext}} \quad (\text{E.7})$$

where

$\bar{e}^i$  is the normal unit vector of  $i$ -th surface element;

$\bar{D}^{ij}$  is the analytical solution of the integral part in Formula (E.5) related to the  $i$ -th and  $j$ -th elements;

$n$  is the number of elements;

$i, j$  is the index from 1 to  $n$ .

By using Formulas (E.2) and (E.3), the demagnetizing factor  $N^S$  derived from the magnetic polarization  $J$  and the demagnetizing factor  $N^V$  derived from the strength of the self-demagnetizing field are written as Formulas (E.8) and (E.9), respectively.

$$N^S = \mu_0 \left( \frac{H_{\text{ext}}}{J} - \frac{1}{\mu_0 \chi} \right) \quad (\text{E.8})$$

$$N^V = \frac{-H_d}{\chi(H_{\text{ext}} + H_d)} \quad (\text{E.9})$$

When the magnetic susceptibility  $\chi$  is given, the magnetic charge density on the surface of the magnet  $\sigma$  can be determined by solving Formula (E.7). The magnetic polarization  $J$  is derived from Formula (E.4) and the self-demagnetizing field strength  $H_d$  is derived from Formula (E.6). Finally, the demagnetizing factors  $N^S$  derived from the magnetic polarization  $J$  and the demagnetizing factor  $N^V$  derived from the strength of the self-demagnetizing field are calculated from Formulas (E.8) and (E.9), respectively.

Formula (E.6) can be numerically solved by using a FEM.

Since generally the demagnetizing factor  $N^S$  derived from the magnetic polarization  $J$  and the demagnetizing factor  $N$  are not equal to the demagnetizing factor  $N^V$  derived from the strength of the self-demagnetizing field, the demagnetizing factor  $N$  is calculated from Formula (E.9).

The demagnetizing factor  $N$  is calculated for any value of the magnetic susceptibility  $\chi$  using Formula (E.10).

$$N = -\frac{\mu_0 H_d}{J} = -\frac{(1 + N^S \chi) H_d}{\chi H_{\text{ext}}} = N^V \frac{1 + N^S \chi}{1 + N^V \chi} \quad (\text{E.10})$$

By this procedure, the relation of the magnetic susceptibility  $\chi$  and demagnetizing factor  $N$  can be found in literature (see Table 1 of [6]).

#### E.4 Method using an inverse analysis considering the spatial distribution of the self-demagnetizing field strength in the test specimen (Method C)

Figure E.2 illustrates a conceptual diagram of the procedure of Method C [7].

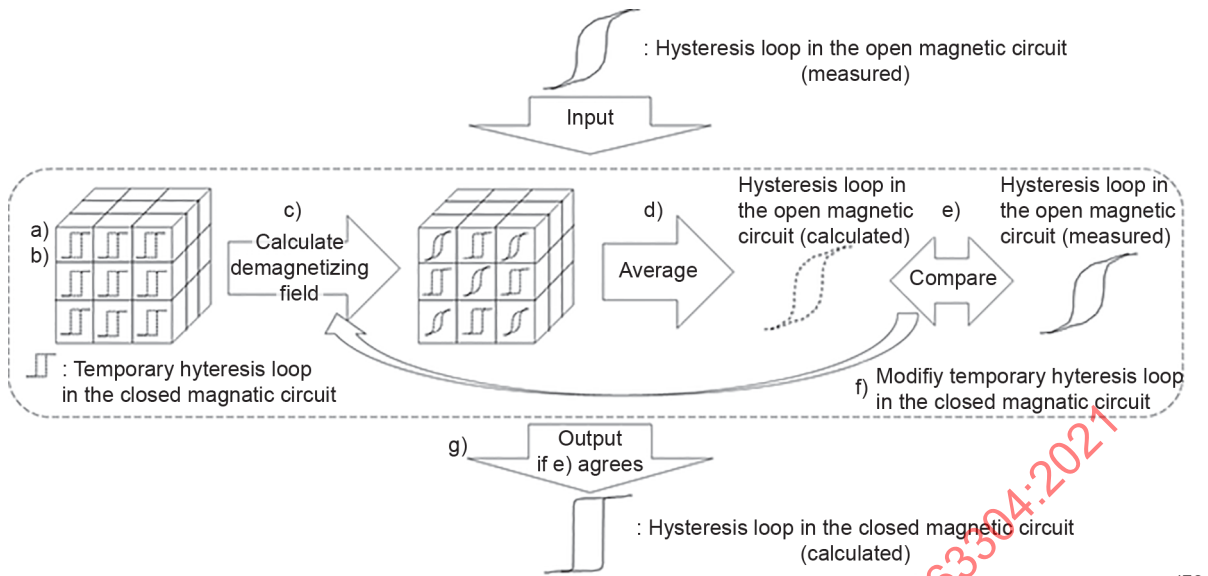


Figure E.2 – Conceptual diagram of the procedure of Method C

The following algorithm is implemented in a computing program and the calculations are executed in a computer. The procedure is written in the flowchart of Figure E.3.

- a) Load a mesh file, e.g. “mesh.dat”, of the magnet model.

The mesh interval is recommended to be more than 10 per dimension of the magnet model so as to consider the spatial distribution of the self-demagnetizing field strength in the magnet model.

- b) Load an input data file, e.g. “Jopen.dat”, of the data set of the butterfly  $J_{\text{open}}^{\text{exp}}(H_{\text{ext}})$  loop obtained by measurement in an open magnetic circuit. The strength of the external magnetic field  $H_{\text{ext}}$  is discretized. The total number of discretization steps of  $H_{\text{ext}}$  is recommended to be more than 300 so as to keep enough calculation accuracy.

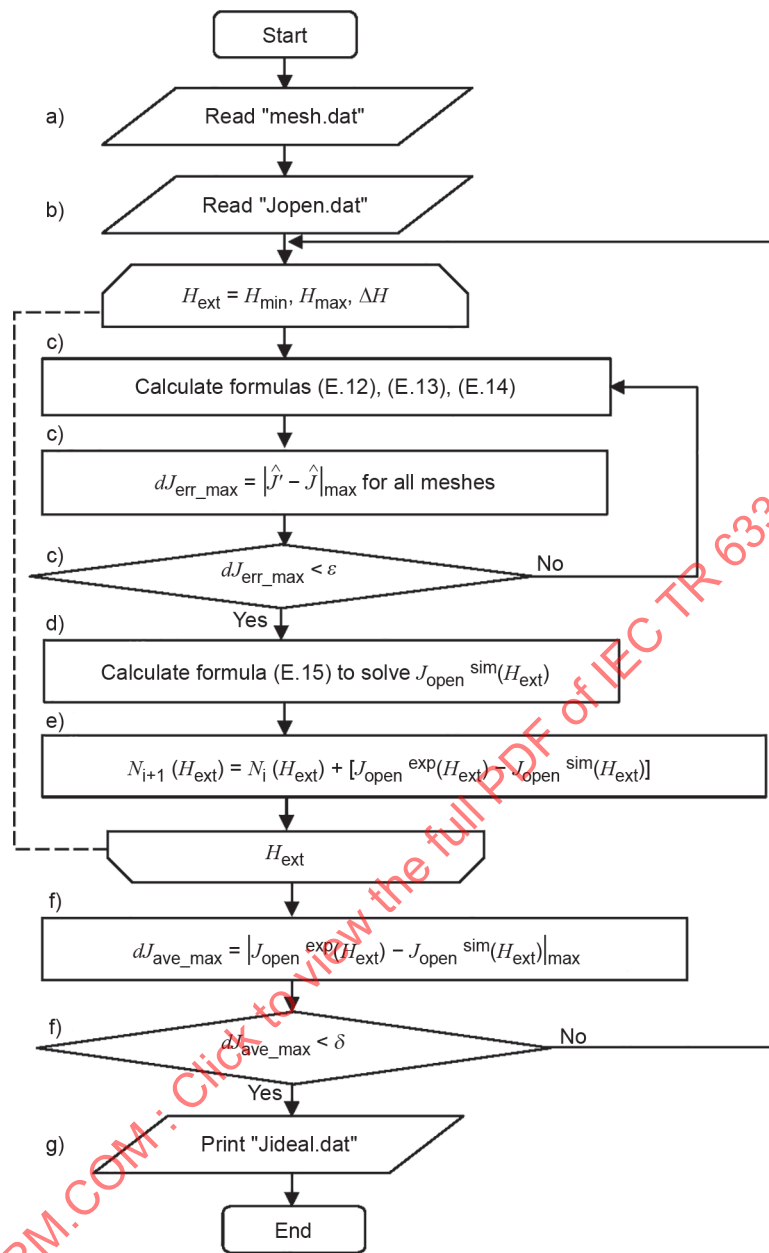
Extract the necessary parameters  $J_r^{\text{exp}}$ ,  $H_c^{\text{exp}}$ ,  $H_{\text{max}}$ , and  $H_{\text{min}}$  for the calculation from the data set.

Set the temporary hysteresis loop  $J_{\text{ideal}}(H)$  defined in Formula (E.11) to all nodes of the mesh.

$$J_{\text{ideal}}(H) = J_r^{\text{exp}} \tanh\left(\mathbf{S} \frac{H - H_c^{\text{exp}}}{1 - N(H)}\right) + \mu_0 (H - H_c^{\text{exp}}) (1 + 0,1N(H)) \quad (\text{E.11})$$

Initialize the value of the parameter  $N(H_{\text{ext}})$  to zero.

- c) Calculate the spatial distribution of the self-demagnetizing field strength  $\hat{H}_d(x, y, z)$  for all nodes of the mesh by using a FEM.



IEC

Figure E.3 – Flowchart of the procedure of Method C

When the spatial distribution of the magnetic polarization  $\hat{j}(x, y, z)$  is given, the spatial distribution of the self-demagnetizing field strength  $\hat{H}_d(x, y, z)$  can be calculated from Formulas (E.12) and (E.13).

$$\hat{H}_d = -\nabla\hat{U} \quad (\text{E.12})$$

$$\nabla^2\hat{U} = \nabla \cdot \frac{\hat{j}}{\mu_0} \quad (\text{E.13})$$

The magnetic polarization at each node  $\hat{J}(x, y, z)$  is calculated using Formula (E.14).

$$\hat{J} = J_{\text{ideal}}(H_{\text{ext}} + \hat{H}_d) \quad (\text{E.14})$$

Repeat calculation of Formulas (E.12) to (E.14) until the maximum value of the residues of the magnetic polarization  $\hat{J}(x, y, z)$ ,  $dJ_{\text{err\_max}}$ , becomes smaller than a predetermined threshold  $\varepsilon$  in order to get self-consistent spatial distributions of the magnetic polarization  $\hat{J}(x, y, z)$  and the self-demagnetizing field strength  $\hat{H}_d(x, y, z)$ . Since the self-demagnetizing field strength has a spatial distribution in the magnet, hysteresis loops at meshes calculated by formula (E.14) are different from each other, as shown in Figure E.2.

- d) Calculate the hysteresis loop  $J_{\text{open}}^{\text{sim}}(H_{\text{ext}})$  of the magnet model by averaging all magnetic polarizations of all meshes using Formula (E.15).

$$J_{\text{open}}^{\text{sim}}(H_{\text{ext}}) = \frac{1}{V} \int_{V_c} J_{\text{ideal}}(H_{\text{ext}} + \hat{H}_d) dV' \quad (\text{E.15})$$

- e) Calculate the difference between the measured hysteresis loop  $J_{\text{open}}^{\text{exp}}(H_{\text{ext}})$  and the calculated hysteresis loop  $J_{\text{open}}^{\text{sim}}(H_{\text{ext}})$  and add the difference into the parameter  $N(H_{\text{ext}})$  using Formula (E.16).

$$N_{i+1}(H_{\text{ext}}) = N_i(H_{\text{ext}}) + u \left[ J_{\text{open}}^{\text{exp}}(H_{\text{ext}}) - J_{\text{open}}^{\text{sim}}(H_{\text{ext}}) \right] \quad (\text{E.16})$$

- f) Calculate the difference in magnetic polarization,  $dJ_{\text{ave\_max}}$ , between the measured hysteresis loop  $J_{\text{open}}^{\text{exp}}(H_{\text{ext}})$  and the calculated hysteresis loop  $J_{\text{open}}^{\text{sim}}(H_{\text{ext}})$  using Formula (E.17).

$$dJ_{\text{ave\_max}} = \left| J_{\text{open}}^{\text{exp}}(H_{\text{ext}}) - J_{\text{open}}^{\text{sim}}(H_{\text{ext}}) \right|_{\text{max}} \quad (\text{E.17})$$

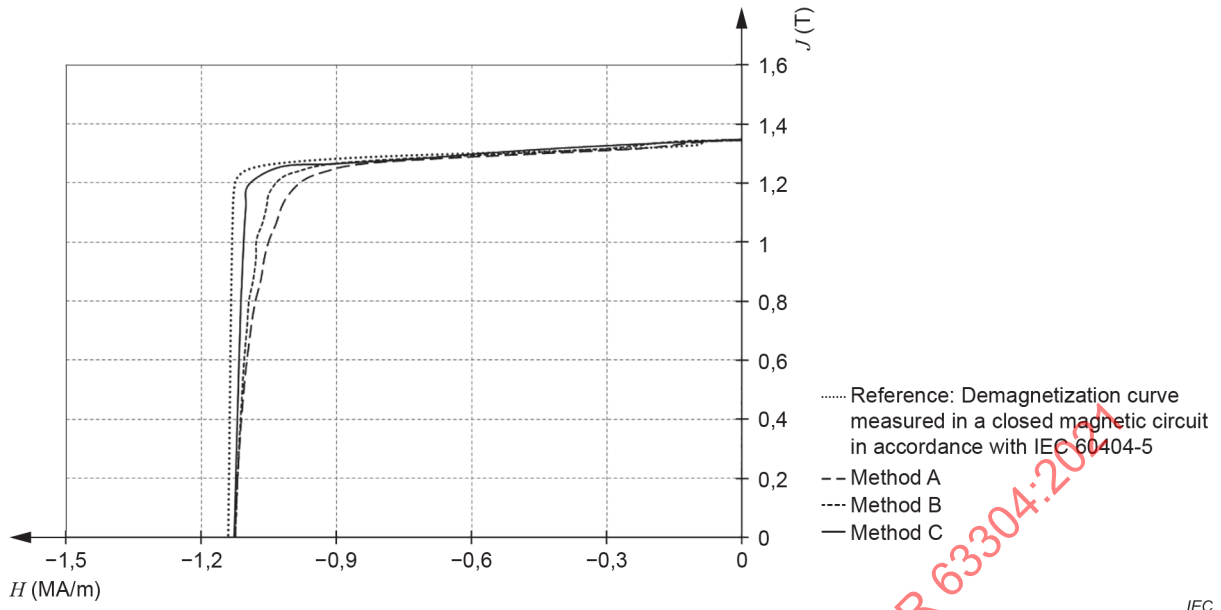
Repeat procedure c) to e) until the value  $dJ_{\text{ave\_max}}$  becomes smaller than a prescribed threshold  $\delta$ .

Finish the calculation if  $dJ_{\text{ave\_max}}$  becomes smaller than the threshold  $\delta$ , and treat the calculated hysteresis loop  $J_{\text{ideal}}(H)$  as the real one.

The calculation accuracy becomes higher as the thresholds  $\delta$  and  $\varepsilon$  decrease, but at the same time the duration becomes longer. That is why it is necessary to set the value of the threshold properly, and in this procedure the values of  $\delta$  and  $\varepsilon$  are recommended to be  $5,0 \times 10^{-2}$  T and  $1,0 \times 10^{-4}$  T, respectively.

- g) Output the data set of the calculated butterfly  $J_{\text{ideal}}(H_{\text{ext}})$  loop into “Jideal.dat”.

The demagnetization curves corrected using different demagnetizing field correction methods are shown in Figure E.4. The squareness of the demagnetization curve corrected using the inverse analysis considering the spatial distribution of the self-demagnetizing field strength (Method C) is the nearest to the demagnetization curve measured in a closed magnetic circuit in accordance with IEC 60404-5.



IEC

**Figure E.4 – Comparison of the demagnetization curves corrected using demagnetizing field correction Methods A, B and C**

IECNORM.COM : Click to view the full PDF of IEC TR 63304:2021